

Article

The Coulomb Symmetry and a Universal Representation of Rydberg Spectral Line Shapes in magnetized Plasmas

Andrei Letunov^{1,2} , Valery Lisitsa*^{1,2}

¹ National Research Centre "Kurchatov institute", 123182 Moscow, Russia nrcki@nrcki.ru

² National Research Nuclear University MEPhI, 115409 Moscow, Russia info@mephi.ru

* vlisitsa@yandex.ru

Abstract: A new method of line shape calculations of hydrogen-like atoms in magnetized plasmas is presented. This algorithm makes it possible to solve two fundamental problems in the broadening theory: the analytical description of the radiation transition array between excited atomic states and account of a thermal ion motion effect on the line shapes formation. The solution to the first problem is based on the semiclassical approach to dipole matrix elements calculations and the usage of the specific symmetry properties of the Coulomb field. The second one is considered in terms of the kinetic treatment of the frequency fluctuation model (FFM). As the result one has a universal description of line shapes under the action of the dynamic of ion's microfield. The final line shape is obtained by the convolution of the ionic line shape with the Voigt electron-Doppler profile. The method is applicable formally for large values of principle quantum numbers. However, it is demonstrated the efficiency of the results even for well known first members of the hydrogen Balmer series D_α and D_β lines. The comparison of obtained results with accurate quantum calculations is presented. The new method may be of interest for investigations of spectral line shapes of hydrogen-like ions presented in different kinds of hot ionized environments with the presence of a magnetic field, including SoL and divertor tokamak plasmas.

Keywords: Stark-Zeeman effect; Rydberg atom; plasma spectroscopy

1. Introduction

Hydrogen spectral lines are of permanent interest both from the fundamental point of view and an applications in plasma diagnostic. Since the middle of the 20th century, a significant number of works and monographs (for example [1–5]) have been accumulated on the spectra of hydrogen plasma. However, the effect of a magnetic field on spectral lines is still remains the problem in plasma diagnostics. Difficulties connected with analysis of the Stark-Zeeman spectra relate to a hydrogen in external crossed **F** electric and **B** magnetic fields.

Calculation of spectral line shape in plasmas is complicated by two serious problems. The first of them is the complex structure of the dipole matrix elements, as well as the rapid growth of the array of radiative transitions. The second one is connected with the problem of the influence of an ion thermal velocity on the intensity profile. This paper shows how one can get around these difficulties. The complex expressions for the probability transitions can be simplified by using the semiclassical approximation for coordinate matrix elements obtained by S.A. Gulyaev [6,7] and specific properties of the Wigner d-functions [8]. The thermal motion of ions can be taken into account using the FFM. It turns out that spectral line shape in plasma with moving ions is the functional of the static profile [9].

The first attempt to provide the solution to this problem was made within the framework of the classical mechanics [10]. The perturbed motion of the electron was reduced to an independent precession of two vectors representing the combination of the angular momentum and the averaged coordinate around two different axes. The quantum approach to this problem has become possible

thanks to the fundamental work of V.A.Fock [11]. The author of this paper showed that an electron in the Coulomb field has enhanced O(4) (instead of common O(3)) symmetry. This fact leads to the existence of two additional constant of motion $J_{1,2}$, which are connected with the orbital momentum \mathbf{l} by the simple relation $\mathbf{l} = \mathbf{J}_1 + \mathbf{J}_2$. A rigorous quantum consideration of this problem is given in [12]. In this work the authors used the O(4) symmetry properties of the Coulomb field to obtain the spectra of a hydrogen atom in the external electric and magnetic fields. The Hamiltonian of this system is equal to

$$H = \frac{\mathbf{p}^2}{2} - \frac{Z}{r} + \mathbf{Fr} + \frac{1}{2c} \mathbf{BL} \quad (1)$$

where \mathbf{p}, \mathbf{r} and \mathbf{L} are the momentum, the coordinate and the angular momentum operators of the electron, correspondingly, Z is the charge of nuclei. This formula and every other in this paper is written in the atomic units. The perturbed part $\mathbf{Fr} + \frac{1}{2c} \mathbf{BL}$ can be rewritten in another way.

$$\Delta H = \mathbf{Fr} + \frac{1}{2c} \mathbf{BL} = \mathbf{E}_1 \mathbf{J}_1 + \mathbf{E}_2 \mathbf{J}_2 \quad (2)$$

where

$$\mathbf{J}_{1,2} = \frac{1}{2} (\mathbf{L} \pm \mathbf{A}) \quad (3)$$

where 1 relates to + and 2 to -;

\mathbf{A} is the specific constant of motion in the Coulomb field - the Runge-Lenz vector.

$$\mathbf{E}_{1,2} = \frac{1}{2c} \mathbf{B} \mp \frac{3}{2} n \mathbf{F} \quad (4)$$

We can do this, because in the Coulomb field there is connection between the Runge-Lenz vector and the coordinate:

$$\mathbf{A} = -\frac{2}{3n} \mathbf{r} \quad (5)$$

The energy shift is equal to

$$\Delta\omega = E_1 n' + E_2 n'' \quad (6)$$

where n' and n'' are projections of (3) on the vectors (4)

Obviously, the vectors (3) are constants of motion in the Coulomb field. Moreover, they have the angular momentum properties. Coming to the parabolic basis there is the connection between the parabolic quantum numbers n_1, n_2 and projections on the single direction [13]

$$\begin{cases} i_2 - i_1 = n_1 - n_2 \\ i_2 + i_1 = m \end{cases} \quad (7)$$

where $i_{1,2}$ are projections of (3) on the z direction (quantization axis), m is the magnetic quantum number.

Using the angular momentum properties of vectors (3) we can express the wave functions in the representation of n, n', n'' in terms of the parabolic states.

$$|n, n', n''\rangle = \sum_{i_1=-j}^j \sum_{i_2=-j}^j d_{i_1 n'}^j(\alpha_1) d_{i_2 n''}^j(\alpha_2) |ni_1 i_2\rangle \quad (8)$$

where $d_{m_1 m_2}^j(\beta)$ is the Wigner d-function.

$$j = \frac{n-1}{2} \quad (9)$$

Here in (8) $\alpha_{1,2}$ are the angles between vectors $\mathbf{J}_{1,2}$ and $\mathbf{E}_{1,2}$. We choose the reference frame, in which, the direction of the magnetic field coincides with the z axis.

$$\cos\alpha_{1,2} = \frac{\frac{1}{2c}B \mp \frac{3}{2}nF\cos\theta}{E_{1,2}} \quad (10)$$

where θ is the angle between electric \mathbf{F} and magnetic fields \mathbf{B} .

The coordinate matrix elements in basis (8) has the following form

$$a_{\bar{n}\bar{n}'\bar{n}''}^{\bar{n}\bar{n}'\bar{n}''} = \sum_{\bar{i}_1=-\bar{j}}^{\bar{j}} \sum_{\bar{i}_2=-\bar{j}}^{\bar{j}} \sum_{i_1=-j}^j \sum_{i_2=-j}^j d_{\bar{i}_1\bar{n}}^{\bar{j}}(\bar{\alpha}_1) d_{\bar{i}_2\bar{n}''}^{\bar{j}}(\bar{\alpha}_2) d_{i_1n'}^j(\alpha_1) d_{i_2n''}^j(\alpha_2) a_{ni_1i_2}^{\bar{n}\bar{i}_1\bar{i}_2} \quad (11)$$

where $a = X, Y, Z$ (The intensity of radiation in the dipole approximation is proportional to the squared absolute value of the coordinate matrix element).

Accurate quantum expressions for the matrix elements $a_{ni_1i_2}^{\bar{n}\bar{i}_1\bar{i}_2}$ in (11) were obtained by Gordon [14,15] and have very complicated structure. They contain the hyper-geometric series which makes calculations for Rydberg atoms very cumbersome. The detailed analysis of computational complexities and ways to get around them are presented in [16]. The array of radiative transitions grows proportionally to n^4 . In order to carry out calculations for highly excited levels the author in [6,7] obtained the approximation of $a_{ni_1i_2}^{\bar{n}\bar{i}_1\bar{i}_2}$ and developed the method of distribution of atomic transitions into special groups. These results and usage of the specific d-functions properties allow one to simplify the complicated expression (11). The results for the $H_{n\alpha}$ ($\Delta n = n - \bar{n} = 1$) and $H_{n\beta}$ ($\Delta n = n - \bar{n} = 2$) series are obtained in [17,18]. The basics of the approach to calculating these matrix elements and the results (see formulas (A11)-(A16)) are presented in the Appendix.

In the present paper we take into account thermal velocity of ions. This problem is closely related to stochastic processes in the Coulomb-like interacting medium. Statistical aspects of the collective motion in the Coulomb field are considered in [19]. The frequency fluctuation model (FFM) consists in the dependence of the spectral line profile on the jumping ion frequency ν .

$$\nu = N_i^{-\frac{1}{3}} v_{Ti} \quad (12)$$

where N_i is the density and v_{Ti} is the thermal velocity of ions.

Using the FFM, the intensity $J(\omega)$ can be analytically expressed as the functional of the normalized static profile $W(\omega)$ [9].

$$J(\omega) = \frac{\nu}{\pi} \frac{J_0(\omega)J_2(\omega) - J_1^2(\omega)}{J_2^2(\omega) + \nu^2 J_1^2(\omega)} \quad (13)$$

$$J_k(\omega) = \int_{-\infty}^{+\infty} \frac{W(\omega')(\omega - \omega')^k}{\nu^2 + (\omega - \omega')^2} d\omega' \quad (14)$$

The similar calculation, using the FFM, but without taking into account the influence of the magnetic field on the shape of spectral lines, is given in [20]. Moreover, this work contains the detailed analysis of the influence of the thermal ion velocity on the plasma line shapes.

The spectral lines profiles in the presence of a magnetic field were calculated in [21]. The authors used the accurate analytical expressions for the dipole matrix elements. However, this work contains profiles only of L_α and D_α lines. Also the authors didn't consider the thermal motion of ions. Application of the frequency-fluctuation model to Stark-Zeeman line shapes was demonstrated in [22]. Again, this work considers only the transitions with small principle number n . Computer modeling, taking into account the largest possible number of effects on the shape of spectral lines, is presented in the works of Rosato et al [23,24].

In the present paper we derive the analytical expressions for spectral lines profiles in plasma. These formulas are convenient for simply performing calculations with them. In fact we provide the

algorithm of spectral lines shapes calculations with given parameters of plasma. The expressions for transitions with $\Delta n = 1$ and $\Delta n = 2$ are presented.

2. Description of the method

Firstly, we will consider the general expression for the plasma spectral line static profile.

$$W(\omega) = \sum_{\tau\rho} \int_0^{+\infty} dF \int d\Omega H(F) |a_{\tau}^{(\rho)}(F, \Omega)|^2 \delta(\omega - \omega_{\tau}(F, \Omega)) \quad (15)$$

where τ is the full set of all quantum numbers related to the initial and final states, ρ is the polarization, $H(F)$ is the distribution function of the absolute value of electric field, Ω defines the angle between the magnetic field and an ion microfield, $a_{\tau}^{(\rho)}(F, \Omega)$ is the dipole matrix element (expressions (A11)-(A13) for $H_{n\alpha}$ and (A14)-(A16) for $H_{n\beta}$ are presented in the Appendix).

Coming up to our notation one will obtain

$$\sum_{\tau} = \sum_{n'=-j}^j \sum_{n''=-j}^j \sum_{\bar{n}'=-\bar{j}}^{\bar{j}} \sum_{\bar{n}''=-\bar{j}}^{\bar{j}}$$

Here values with bar relate to the final state.

In the ρ summation there are only two terms. For example if one calculate the radiation intensity with direction of observation parallel to magnetic field ρ will correspond to X and Y directions. In other words, in this example one have to put $a^{(1)} = X$ and $a^{(2)} = Y$.

In (15) $\delta(z)$ is the Dirac delta-function and $\omega_{\tau}(E, \Omega)$ is the energy shift that corresponds to the set of quantum numbers τ . In our case we have

$$\omega_{\tau}(F, \theta) = \bar{E}_1(F, \theta) \bar{n}' + \bar{E}_2(F, \theta) \bar{n}'' - E_1(F, \theta) n' - E_2(F, \theta) n'' \quad (16)$$

Here we used the absolute values of the vectors (4). The fact that the system has the circular symmetry is also used, which means that there is no dependence of the energy shift and the matrix elements on the azimuthal angle.

As $H(F)$ one can use the Holtsmark distribution

$$H(F) = \frac{2}{\pi F} \int_0^{\infty} x \sin x \exp \left[-\left(\frac{xF_0}{F} \right)^{\frac{3}{2}} \right] dx \quad (17)$$

$$F_0 = 2.6031 Z_i N_i^{\frac{2}{3}} \quad (18)$$

where Z_i is the charge and N_i is the density of ions. The detailed analysis of the Holtsmark distribution is presented in [5,19].

To take into account the thermal velocity of ions in plasmas we will use formulas (13) and (14). One can substitute the expression (15) into (14). After that it is possible to integrate over ω' and get rid of the delta functions.

$$J_k(\omega) = \sum_{\tau\rho} \int_0^{+\infty} dF \int d\Omega H(F) |a_{\tau}^{(\rho)}(F, \Omega)|^2 \frac{(\omega - \omega_{\tau}(F, \Omega))^k}{\nu^2 + (\omega - \omega_{\tau}(F, \Omega))^2} \quad (19)$$

Now it is necessary to take into account the Doppler and the electron broadening mechanisms. In order to do this one have to calculate the convolution of $J(\omega)$ from (13) (With J_k from (19)) with the Voigt profile

$$V(\omega, D, \gamma) = \int_{-\infty}^{+\infty} F(\omega', D) U(\omega - \omega', \gamma) d\omega' \quad (20)$$

$$F(\omega, D) = \frac{1}{\sqrt{\pi D}} \text{Exp} \left[- \left(\frac{\omega}{D} \right)^2 \right] \quad (21)$$

Expression (21) relates to the Doppler broadening [5]. Here D is the Doppler parameter

$$D = \frac{\omega_{n\bar{n}}}{c} \sqrt{\frac{2T_a}{M}} \quad (22)$$

where $\omega_{n\bar{n}} = \frac{Z^2}{2} \left(\frac{1}{n^2} - \frac{1}{\bar{n}^2} \right)$, c is the speed of light in vacuum, M and T_a are the mass and temperature of atoms, correspondingly.

$$U(\omega, \gamma) = \frac{\gamma}{\pi} \frac{1}{(\frac{\gamma}{2})^2 + \omega^2} \quad (23)$$

That Lorentz distribution corresponds to the electron broadening. Generally, calculation of the parameter γ is complicated process. We will use the simplified approach to the electron broadening(see [5]).

$$\gamma = 16N_e v_{Te} \rho_0^2 \left[0.33 + \ln \frac{\rho_m}{\rho_0} \right] \quad (24)$$

where N_e and v_{Te} are the density and thermal velocity of electrons, correspondingly, ρ_m is the Debye radius in plasmas.

$$\rho_0^2 = \frac{2}{3v_{Te}^2} I(n, \bar{n}) \quad (25)$$

$$I(n, \bar{n}) = 2 \left(\sum_{ab} |\mathbf{P}_{ab}|^2 \right)^{-1} \sum_{aa'bb'} \mathbf{P}_{a'b'} \mathbf{P}_{ba} \left(\delta_{bb'} \sum_{a''} \mathbf{r}_{aa''} \mathbf{r}_{a''a'} + \delta_{aa'} \sum_{b''} \mathbf{r}_{b'b''} \mathbf{r}_{b''b} - 2 \mathbf{r}_{aa'} \mathbf{r}_{b'b} \right) \quad (26)$$

where \mathbf{r} is the coordinate operator, $|\mathbf{P}_{ab}|^2$ is the transition intensity, a and b denote different states referring to levels n, \bar{n} . For example:

$$I(n, 1) = \frac{9}{4} n^2 (n^2 - 3)$$

$$I(n, 2) = \frac{9}{4} (n^4 - 9n^2 + 12)$$

$$I(n, 3) = \frac{9}{4} (n^4 - 19n^2 + 72)$$

More accurate calculations for the electron broadening are discussed in [25]. Moreover, modification of this broadening theory is presented in the Appendix of [21].

Finally, we can obtain the formula for the intensity of radiation as the function of the energy shift(frequency). It is the convolution of the expressions (13) and (20).

$$I(\omega) = \int_{-\infty}^{+\infty} J(\omega') V(\omega - \omega', D, \gamma) d\omega' \quad (27)$$

To sum all up, we obtained the algorithm for plasma line shapes calculations. Expressions for the dipole matrix elements are presented in the Appendix. We have taken into account Stark, Zeeman, Doppler and electron mechanisms of broadening. Moreover, using the FFM, the effect of thermal velocity is considered. For every step of calculation we used analytical expressions. The approximations for the transitions intensities are derived for lines with $\Delta n = n - \bar{n} = 1$ and $\Delta n = 2$. Main advantage this method is the opportunity of making calculations for any large principle numbers.

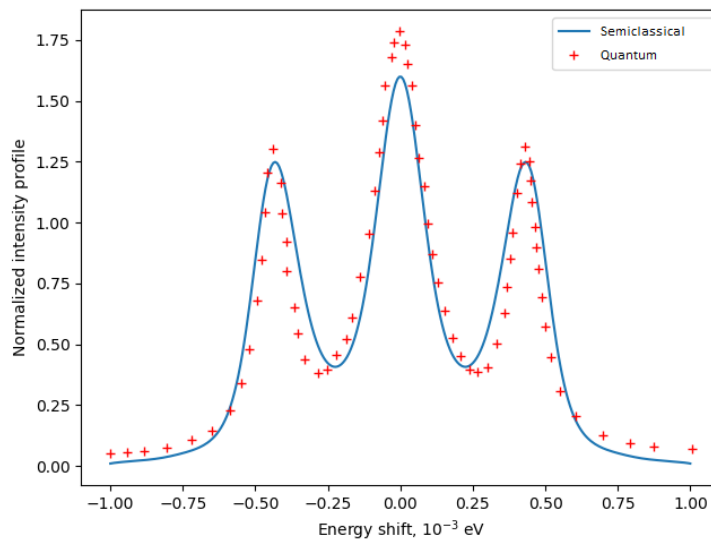


Figure 1. Normalized intensity profile of D_α spectral line (transition 3-2) as the function of the energy shift. The direction of observation is perpendicular to the magnetic field, $T_e = T_i = 1\text{ eV}$, $N_i = N_e = 10^{15}\text{ cm}^{-3}$, $B = 7\text{ T}$. The comparison of the semiclassical approach and accurate calculation from [22].

3. Results

Specific calculations for deuterium plasma are demonstrated in this section of the present paper. In order to estimate accuracy of the method we compare the results of other groups for the D_α and D_β spectral lines with our algorithm.

The comparison of semiclassical calculations and the results from [22] are presented in figure 1. One can observe the satisfactory correspondence between two approaches. Even for low levels $n = 2$ and $n = 3$ the Rydberg approximation shows high degree of accuracy. However, there is a slight discrepancy, mainly due to the imprecision in the calculations of the Stark shift. This calculation is extremely representative because in both approaches the thermal velocity of ions is taken into account in the same way. In fact, the main difference here is the choice of expressions for the transition probabilities.

One can observe tolerable coincidence between the Rydberg approach to spectral lines in plasmas and the computer modelling from [24]. Calculations for D_β line are presented in figure 2. The semiclassical approach is distinguished by a narrowing in the center. It is connected with widening on the sides. The reason for these little 'wings' is Zeeman components. Inaccuracy of the Rydberg approximation leads to a slight decrease in the Stark shift. However, this result should be considered quite satisfactory because distance between atomic levels is equal to principle quantum number of a lower state.

Obviously, with growth of n the Rydberg approximation will be practically indistinguishable from the exact result. For large values of the principle quantum number distance between atomic levels $\Delta n \ll n$, so it won't influence on the Stark shift. Moreover, electron broadening parameter $\gamma \sim n^4$ (except specific cases of interference of contributions to the electron width, the details can be found in [4]). For highly excited levels the electron impact to the broadening can blur spectral lines. Thus, the small inexactness connected with the Rydberg approximation can all the more be neglected.

4. Conclusion

The semiclassical approach to the spectral lines in plasmas is presented. We demonstrated how one can use the analytical expressions for calculating $H_{n\alpha}$ and $H_{n\beta}$ line shapes. Thanks to the presented

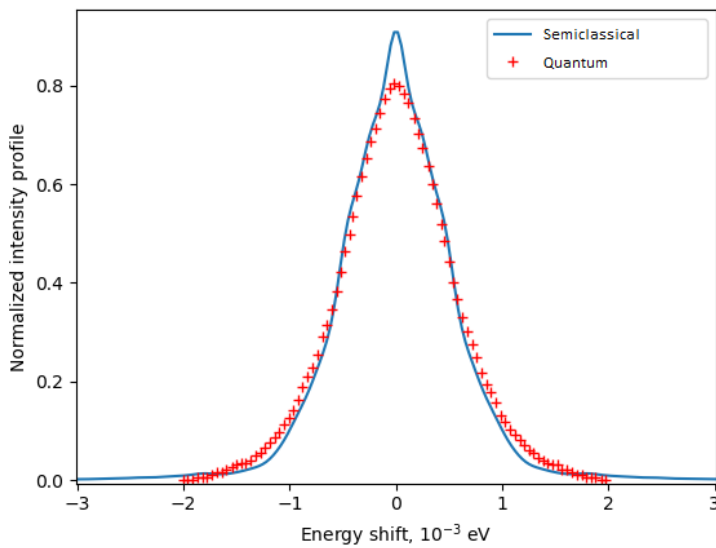


Figure 2. Normalized intensity profile of D_β spectral line (transition 4-2) as the function of the energy shift. Direction of observation perpendicular to magnetic field, $T_e = T_i = 1\text{eV}$, $N_i = N_e = 10^{15}\text{cm}^{-3}$, $B = 5\text{T}$. The comparsion of the semiclassical approach and the computer modelling from [24].

method, it is possible to calculate the intensity profiles for transitions with a large principle quantum numbers. Basically, this approach is suitable to the spectral line shapes of hydrogen-like ions. For calculations within the visible range, it is necessary to consider transitions with larger n . Moreover, it was shown that this approach can be used to achieve satisfactory agreement with the transitions related to the Balmer series (fig. 1,2).

Using the FFM, one can relatively simply take into account the effect of the thermal motion of ions in the plasma on the shape of spectral lines. The FFM profile depend on the functions $J_k(\omega)$ (14). Integrant in $J_k(\omega)$ depends on static profile $W(\omega)$ (15). The function $W(\omega)$ expressed in terms of the delta-functions. It allows one do a simple integration and obtain formula (19) for $J_k(\omega)$.

In [12] the authors consider a Hydrogen atom in external crossed electric \mathbf{F} and magnetic \mathbf{B} fields. They performed calculations in the specific basis (8). These states are closely related to the parabolic quantization on two different axes. Calculation of the transition probabilities in this basis leads one to formula (11). Using the symmetry properties of the Coulomb field, the Wigner d-functions recurrence relations and the Rydberg asymptotic formulas for the coordinate matrix elements [6,7], the simple semiclassical approximations for the dipole matrix elements in representation of states (8) were obtained in (LL) and applied to the spectral line shape calculations. The approximations for the transitions probabilities in this basis are presented in the Appendix (see (A11)-(A16)).

To demonstrate the power of the Rydberg atom approach, Balmer series line shapes were calculated and compared with the results of other groups. Shape of D_α line is presented in figure 1. One can observe good correspondence with accurate consideration from [22]. Comparsion of Rydberg approach and the computer simulation [24] is presented in the figure 2. Even for the 4 – 2 transition the analytical approximation shows good correspondence with quantum calculations.

Appendix A Dipole matrix elements

The detailed derivation of the semiclassical approximation of the dipole matrix elements is the representation of states (8) is presented in [17,18]. In the appendix, we will briefly discuss the main

points of calculating the transition probabilities and present the results from works [17,18]. Firstly, it is necessary to consider new quantum number K

$$K = (n_1 - n_2) - (\bar{n}_1 - \bar{n}_2) \quad (A1)$$

It turns out that the a radiative transition probability strongly depends on this number (A1) [6,7]. It partially solves the problem of a large array of transitions between Rydberg atomic states. It is necessary to calculate the intensity of transitions only with a certain value of K. For example, while calculating the spectral line shape of the $H_{n\alpha}$ line one have to calculate transitions only with $K = 0$ and $K = \pm 1$. By fixing the magnetic quantum number m and K it is possible to establish the approximate selection rules for the parabolic quantum numbers (7)

For Z matrix element ($\Delta n = 1$)

$$\begin{cases} (i_2 - i_1) - (\bar{i}_2 - \bar{i}_1) = \pm 1 \\ i_2 + i_1 = \bar{i}_2 + \bar{i}_1 \end{cases} \quad (A2)$$

For X-matrix element ($\Delta n = 1$)

$$\begin{cases} (i_2 - i_1) - (\bar{i}_2 - \bar{i}_1) = 0 \\ |i_2 + i_1| = |\bar{i}_2 + \bar{i}_1| \pm 1 \end{cases} \quad (A3)$$

In the case of $H_{n\beta}$ line it is necessary to calculate the dipole matrix elements with $K = \pm 1$ and $K = \pm 2$. Similar systems can be written for the case $\Delta n = 2$.

For Z matrix element ($\Delta n = 2$)

$$\begin{cases} (i_2 - i_1) - (\bar{i}_2 - \bar{i}_1) = \pm 2 \\ i_2 + i_1 = \bar{i}_2 + \bar{i}_1 \end{cases} \quad (A4)$$

For X-matrix element ($\Delta n = 2$)

$$\begin{cases} (i_2 - i_1) - (\bar{i}_2 - \bar{i}_1) = \pm 1 \\ |i_2 + i_1| = |\bar{i}_2 + \bar{i}_1| \pm 1 \end{cases} \quad (A5)$$

By solving systems (A2-A5) we can express $i_{1,2}$ in terms $\bar{i}_{1,2}$. It leads to the reduction of the expression (11) to double sums. Moreover, as it was shown in [17,18], these sums are independent.

For example, solution to the system (A2) reduces the expression (11) to the following formula

$$Z_{nn'n''}^{\bar{n}\bar{n}'\bar{n}''} = Z_{1nn'n''}^{\bar{n}\bar{n}'\bar{n}''} + Z_{2nn'n''}^{\bar{n}\bar{n}'\bar{n}''} \quad (A6)$$

$$Z_{1,2nn'n''}^{\bar{n}\bar{n}'\bar{n}''} = \sum_{\bar{i}_1=-\bar{j}}^{\bar{j}} \sum_{\bar{i}_2=-\bar{j}}^{\bar{j}} d_{\bar{i}_1\bar{n}'}^{\bar{j}}(\alpha_1) d_{\bar{i}_2\bar{n}''}^{\bar{j}}(\alpha_2) d_{\bar{i}_1 \pm \frac{1}{2}n'}^{\bar{j}}(\alpha_1) d_{\bar{i}_2 \mp \frac{1}{2}n''}^{\bar{j}}(\alpha_2) G_{1,2}(\bar{i}_1, \bar{i}_2) \quad (A7)$$

Where

$$G_1 = \sqrt{\left(\frac{n}{2} - \bar{i}_1\right)\left(\frac{n}{2} + \bar{i}_2\right)}$$

$$G_2 = \sqrt{\left(\frac{n}{2} + \bar{i}_1\right)\left(\frac{n}{2} - \bar{i}_2\right)}$$

Formulas for $a_{n\bar{i}_1\bar{i}_2}^{\bar{n}\bar{i}_1\bar{i}_2}$ one can find in [6,7]. Detailed derivation of this expression is presented in [17]. The next step is the usage of the recurrence and orthogonality relations for the Wigner d-functions [8]

$$d_{m_1, m_2}^j(\beta) = \sqrt{\frac{j-m_2}{j-m_1}} \cos\left(\frac{\beta}{2}\right) d_{m_1+\frac{1}{2}, m_2+\frac{1}{2}}^{j-\frac{1}{2}}(\beta) - \sqrt{\frac{j+m_2}{j-m_1}} \sin\left(\frac{\beta}{2}\right) d_{m_1+\frac{1}{2}, m_2-\frac{1}{2}}^{j-\frac{1}{2}}(\beta) \quad (A8)$$

$$d_{m_1, m_2}^j(\beta) = \sqrt{\frac{j-m_2}{j-m_1}} \sin\left(\frac{\beta}{2}\right) d_{m_1-\frac{1}{2}, m_2+\frac{1}{2}}^{j-\frac{1}{2}}(\beta) + \sqrt{\frac{j+m_2}{j-m_1}} \cos\left(\frac{\beta}{2}\right) d_{m_1-\frac{1}{2}, m_2-\frac{1}{2}}^{j-\frac{1}{2}}(\beta) \quad (\text{A9})$$

$$\sum_{m_3=-j}^j (-1)^{m_3-m_2} d_{m_2, m_3}^j(\beta) d_{m_3, m_1}^j(\beta) = \delta_{m_1, m_2} \quad (\text{A10})$$

In both cases of the $H_{n\alpha}$ and $H_{n\beta}$ spectral lines these manipulations leads to the following results
For the $H_{n\alpha}$ line

$$Z_{nn'n''}^{\bar{n}\bar{n}'\bar{n}''} = (-1)^{\Delta\bar{n}'+\Delta\bar{n}''} \frac{1}{4} b \left[Z_{nn'n''}^{(1)\bar{n}\bar{n}'\bar{n}''} + Z_{nn'n''}^{(2)\bar{n}\bar{n}'\bar{n}''} \right] \quad (\text{A11})$$

$$Z_{nn'n''}^{(1)\bar{n}\bar{n}'\bar{n}''} = \left(\sqrt{\frac{n}{2} - n'} \cos \frac{\alpha_1}{2} \delta_{\bar{n}', n'+1/2} - \sqrt{\frac{n}{2} + n'} \sin \frac{\alpha_1}{2} \delta_{\bar{n}', n'-1/2} \right) \times \\ \times \left(\sqrt{\frac{n}{2} - n''} \sin \frac{\alpha_2}{2} \delta_{\bar{n}'', n''+1/2} + \sqrt{\frac{n}{2} + n''} \cos \frac{\alpha_2}{2} \delta_{\bar{n}'', n''-1/2} \right)$$

$$Z_{nn'n''}^{(2)\bar{n}\bar{n}'\bar{n}''} = \left(\sqrt{\frac{n}{2} - n'} \sin \frac{\alpha_1}{2} \delta_{\bar{n}', n'+1/2} + \sqrt{\frac{n}{2} + n'} \cos \frac{\alpha_1}{2} \delta_{\bar{n}', n'-1/2} \right) \times \\ \times \left(\sqrt{\frac{n}{2} - n''} \cos \frac{\alpha_2}{2} \delta_{\bar{n}'', n''+1/2} - \sqrt{\frac{n}{2} + n''} \sin \frac{\alpha_2}{2} \delta_{\bar{n}'', n''-1/2} \right) \\ X_{nn'n''}^{\bar{n}\bar{n}'\bar{n}''} = (-1)^{\Delta\bar{n}'\Delta\bar{n}''-1} \frac{1}{4} b \left[X_{nn'n''}^{(1)\bar{n}\bar{n}'\bar{n}''} - X_{nn'n''}^{(2)\bar{n}\bar{n}'\bar{n}''} \right] \quad (\text{A12})$$

$$X_{nn'n''}^{(1)\bar{n}\bar{n}'\bar{n}''} = \left(\sqrt{\frac{n}{2} - n'} \sin \frac{\alpha_1}{2} \delta_{\bar{n}', n'+1/2} + \sqrt{\frac{n}{2} + n'} \cos \frac{\alpha_1}{2} \delta_{\bar{n}', n'-1/2} \right) \times \\ \times \left(\sqrt{\frac{n}{2} - n''} \sin \frac{\alpha_2}{2} \delta_{\bar{n}'', n''+1/2} + \sqrt{\frac{n}{2} + n''} \cos \frac{\alpha_2}{2} \delta_{\bar{n}'', n''-1/2} \right)$$

$$X_{nn'n''}^{(2)\bar{n}\bar{n}'\bar{n}''} = \left(\sqrt{\frac{n}{2} - n'} \cos \frac{\alpha_1}{2} \delta_{\bar{n}', n'+1/2} - \sqrt{\frac{n}{2} + n'} \sin \frac{\alpha_1}{2} \delta_{\bar{n}', n'-1/2} \right) \times \\ \times \left(\sqrt{\frac{n}{2} - n''} \cos \frac{\alpha_2}{2} \delta_{\bar{n}'', n''+1/2} - \sqrt{\frac{n}{2} + n''} \sin \frac{\alpha_2}{2} \delta_{\bar{n}'', n''-1/2} \right)$$

The hydrogen wave function is proportional to $e^{im\varphi}$, $X \sim \cos\varphi, Y \sim \sin\varphi$. Using well-known relations $\cos(z) = \frac{e^{iz} + e^{-iz}}{2}$ and $\sin(z) = \frac{e^{iz} - e^{-iz}}{2i}$ one can obtain

$$Y_{nn'n''}^{\bar{n}\bar{n}'\bar{n}''} = (-1)^{\Delta\bar{n}' + \Delta\bar{n}'' - 1} \frac{1}{4i} b \left[X_{nn'n''}^{(1)\bar{n}\bar{n}'\bar{n}''} + X_{nn'n''}^{(2)\bar{n}\bar{n}'\bar{n}''} \right] \quad (\text{A13})$$

For the $H_{n\beta}$ line

$$Z_{nn'n''}^{\bar{n}\bar{n}'\bar{n}''} = \frac{1}{4} b (-1)^{\Delta\bar{n}'+\Delta\bar{n}''} \left[Z_{1nn'n''}^{\bar{n}\bar{n}'\bar{n}''} - Z_{2nn'n''}^{\bar{n}\bar{n}'\bar{n}''} \right] \quad (\text{A14})$$

$$Z_{1nn'n''}^{\bar{n}\bar{n}'\bar{n}''} = \left[\left(\frac{n}{2} - n' \right) \cos^2 \left(\frac{\alpha_1}{2} \right) \delta_{\bar{n}', n'+1} - \sin(\alpha_1) \sqrt{\left(\frac{n}{2} - n' \right) \left(\frac{n}{2} + n' \right)} \delta_{\bar{n}', n'} + \right. \\ \left. + \left(\frac{n}{2} + n' \right) \sin^2 \left(\frac{\alpha_1}{2} \right) \delta_{\bar{n}', n'-1} \right] \times \left[\left(\frac{n}{2} - n'' \right) \sin^2 \left(\frac{\alpha_2}{2} \right) \delta_{\bar{n}'', n''+1} + \right. \\ \left. + \sin(\alpha_2) \sqrt{\left(\frac{n}{2} - n'' \right) \left(\frac{n}{2} + n'' \right)} \delta_{\bar{n}'', n''} + \left(\frac{n}{2} + n'' \right) \cos^2 \left(\frac{\alpha_2}{2} \right) \delta_{\bar{n}'', n''-1} \right]$$

$$\begin{aligned}
Z_{2nn'n''}^{\bar{n}\bar{n}'\bar{n}''} = & \left[\left(\frac{n}{2} - n'' \right) \cos^2 \left(\frac{\alpha_2}{2} \right) \delta_{\bar{n}'', n''+1} - \sin(\alpha_2) \sqrt{\left(\frac{n}{2} - n'' \right) \left(\frac{n}{2} + n'' \right)} \delta_{\bar{n}'', n''} + \right. \\
& \left. + \left(\frac{n}{2} + n'' \right) \sin^2 \left(\frac{\alpha_2}{2} \right) \delta_{\bar{n}'', n''-1} \right] \times \left[\left(\frac{n}{2} - n' \right) \sin^2 \left(\frac{\alpha_1}{2} \right) \delta_{\bar{n}', n'+1} + \right. \\
& \left. + \sin(\alpha_1) \sqrt{\left(\frac{n}{2} - n' \right) \left(\frac{n}{2} + n' \right)} \delta_{\bar{n}', n'} + \left(\frac{n}{2} + n'' \right) \cos^2 \left(\frac{\alpha_1}{2} \right) \delta_{\bar{n}', n'-1} \right] \\
X_{nn'n''}^{\bar{n}\bar{n}'\bar{n}''} = & \frac{1}{4} b(-1)^{\Delta\bar{n}'+\Delta\bar{n}''} \left[X_{1nn'n''}^{\bar{n}\bar{n}'\bar{n}''} - X_{2nn'n''}^{\bar{n}\bar{n}'\bar{n}''} - X_{3nn'n''}^{\bar{n}\bar{n}'\bar{n}''} + X_{4nn'n''}^{\bar{n}\bar{n}'\bar{n}''} \right] \quad (A15)
\end{aligned}$$

$$\begin{aligned}
X_{1nn'n''}^{\bar{n}\bar{n}'\bar{n}''} = & \left[\left(\frac{n}{2} - n' \right) \cos^2 \left(\frac{\alpha_1}{2} \right) \delta_{\bar{n}', n'+1} - \sin(\alpha_1) \sqrt{\left(\frac{n}{2} - n' \right) \left(\frac{n}{2} + n' \right)} \delta_{\bar{n}', n'} + \right. \\
& \left. + \left(\frac{n}{2} + n' \right) \sin^2 \left(\frac{\alpha_1}{2} \right) \delta_{\bar{n}', n'-1} \right] \times \left[\frac{1}{2} \sin(\alpha_2) \left(\left(\frac{n}{2} - n'' \right) \delta_{\bar{n}'', n''+1} - \left(\frac{n}{2} + n'' \right) \delta_{\bar{n}'', n''-1} \right) + \right. \\
& \left. + \delta_{\bar{n}'', n''} \cos(\alpha_2) \sqrt{\left(\frac{n}{2} + n'' \right) \left(\frac{n}{2} - n'' \right)} \right] \\
X_{2nn'n''}^{\bar{n}\bar{n}'\bar{n}''} = & \left[\left(\frac{n}{2} - n'' \right) \sin^2 \left(\frac{\alpha_2}{2} \right) \delta_{\bar{n}'', n''+1} + \sin(\alpha_2) \sqrt{\left(\frac{n}{2} - n'' \right) \left(\frac{n}{2} + n'' \right)} \delta_{\bar{n}'', n''} + \right. \\
& \left. + \left(\frac{n}{2} + n'' \right) \cos^2 \left(\frac{\alpha_2}{2} \right) \delta_{\bar{n}'', n''-1} \right] \times \left[\frac{1}{2} \sin(\alpha_1) \left(\left(\frac{n}{2} - n' \right) \delta_{\bar{n}', n'+1} - \left(\frac{n}{2} + n' \right) \delta_{\bar{n}', n'-1} \right) + \right. \\
& \left. + \delta_{\bar{n}', n'} \cos(\alpha_1) \sqrt{\left(\frac{n}{2} + n' \right) \left(\frac{n}{2} - n' \right)} \right]
\end{aligned}$$

Here, $X_{3nn'n''}^{\bar{n}\bar{n}'\bar{n}''}$ can be obtained by switching $n' \Leftrightarrow n''$ (for bar values too) and $\alpha_1 \Leftrightarrow \alpha_2$ in $X_{1nn'n''}^{\bar{n}\bar{n}'\bar{n}''}$. The same connection exists between $X_{2nn'n''}^{\bar{n}\bar{n}'\bar{n}''}$ and $X_{4nn'n''}^{\bar{n}\bar{n}'\bar{n}''}$.

$$Y_{nn'n''}^{\bar{n}\bar{n}'\bar{n}''} = \frac{1}{4i} b(-1)^{\Delta\bar{n}'+\Delta\bar{n}''} \left[X_{1nn'n''}^{\bar{n}\bar{n}'\bar{n}''} - X_{2nn'n''}^{\bar{n}\bar{n}'\bar{n}''} - X_{3nn'n''}^{\bar{n}\bar{n}'\bar{n}''} + X_{4nn'n''}^{\bar{n}\bar{n}'\bar{n}''} \right] \quad (A16)$$

The presence of the delta-functions in formulas (A11)-(A16) expresses the selection rule for the angular momentum. The quantum number corresponding to the angular momentum cannot change by more than 1. Moreover, the presence of delta functions partially solves the problem of the giant array of Rydberg radiative transitions.

References

1. Griem, H. R. *Principles of plasma spectroscopy*. Vol. 2. Cambridge University Press, 2005.
2. Lisitsa, V. S. *Atoms in plasmas*. Vol. 14. Springer Science and Business Media, 2012.
3. Oks, E.A. *Plasma Spectroscopy: The Influence of Microwave and Laser Fields*. Vol. 9. Springer Science and Business Media, 2012.
4. Sobel'Man, I. I., Vainshtein, L.A. and Yukov E. A. *Excitation of atoms and broadening of spectral lines*. Vol. 15. Springer Science and Business Media, 2012.
5. Sobel'Man, I. I. *Introduction to the Theory of Atomic Spectra: International Series of Monographs in Natural Philosophy*. Vol. 40. Elsevier, 2016.
6. Gulyaev, S.A. *Profile of the Hn alpha. radio lines in a static ion field*. Sov. Astron. AJ (Engl. Transl.) 1976, 20. Available online: <http://adsabs.harvard.edu/full/1976SvA....20..573G>.
7. Gulyaev, S.A. *Profile of the Hn beta. radio lines in a static ion field*. Sov. Astron. 1978, 22 Available online: <http://adsabs.harvard.edu/full/1978SvA....22..572G>

8. Varshalovich, D.A., Moskalev, A.N. , Khersonskii, V.K. *Quantum Theory of Angular Momentum: Irreducible Tensors, Spherical Harmonics, Vector Coupling Coefficients, nj Symbols*; World Scientific: Singapore, 2008.
9. Bureeva, L. A., Kadomtsev, M. B., Levashova, M. G., Lisitsa, V. S., Calisti, A., Talin, B., and Rosmej, F. 2010. Equivalence of the method of the kinetic equation and the fluctuating-frequency method in the theory of the broadening of spectral lines. *JETP letters*, 90(10), 647-650.
10. Born, M., Friedrich Hund, and Pascual Jordan. *Vorlesungen über Atommechanik. Vol. 1.* Berlin: Springer, 1925.
11. Fock, V.A. "Zur theorie des wasserstoffatoms." *Zeitschrift für Physik* 98.3-4 1935: 145-154.
12. Demkov, Yu N., Monozon B.S, and Ostrovsky V.N. "Energy levels of a hydrogen atom in crossed electric and magnetic fields." *Sov. Phys. JETP* 30 (1970): 775-776. Available online: http://www.jetp.ac.ru/cgi-bin/dn/e_030_04_0775.pdf.
13. Landau, L. D., and Lifshitz E. M. *Quantum mechanics: non-relativistic theory. Vol. 3.* Elsevier, 2013.
14. Gordon, W. "Zur berechnung der matrizen beim wasserstoffatom." *Annalen der Physik* 394.8 (1929): 1031-1056.
15. Bete, H.A.; Solpiter, E.E. *Quantum Mechanics of Atoms with One and Two Electrons*; Pizmatgiz: Moscow, Russia, 1960.
16. Dewangan, D. P. "An accurate quantum expression of the z-dipole matrix element between nearby Rydberg parabolic states and the correspondence principle." *Journal of Physics B: Atomic, Molecular and Optical Physics* 41.1 2007: 015002. Available online: https://iopscience.iop.org/article/10.1088/0953-4075/41/1/015002/pdf?casa_token=YzHJt4E7TvkAAAAA:pEB1rzYK6W0mwoFCADPwuY3fdz94txO25FJxgr5AHv2ib8Ir1g0BrguJfRYrFJjWV29bhHR2VZA.
17. Letunov A.Yu, Lisitsa V.S. "Stark-Zeeman and Blokhincev spectra of Rydberg atoms". *Journal of theoretical and experimental physics* (2020):131,5(11). Available online: <http://www.jetp.ac.ru/cgi-bin/r/index/r/158/5/p800?a=list>.
18. Letunov, A.Yu, and Lisitsa V.S. "Spectra of a Rydberg Atom in Crossed Electric and Magnetic Fields." *Universe* 6.10 (2020): 157. Available online: <https://www.mdpi.com/2218-1997/6/10/157>.
19. Chandrasekhar, S. "Stochastic problems in physics and astronomy." *Reviews of modern physics* 15.1 (1943): 1.
20. Mossé, C., et al. "A universal approach to Rydberg spectral line shapes in plasmas." *Journal of Physics B: Atomic, Molecular and Optical Physics* 37.6 2004: 1343.
21. Novikov, V. G., et al. "Effect of a magnetic field on the radiation emitted by a nonequilibrium hydrogen and deuterium plasma." *Journal of Experimental and Theoretical Physics* 92.3 2001: 441-453.
22. Ferri, S., et al. "Frequency-fluctuation model applied to Stark-Zeeman spectral line shapes in plasmas." *Physical Review E* 84.2 (2011): 026407.
23. Rosato, J., et al. "A table of Balmer gamma line shapes for the diagnostic of magnetic fusion plasmas." *Journal of Quantitative Spectroscopy and Radiative Transfer* 165 2015: 102-107. Available online: http://www.euro-fusionscipub.org/wp-content/uploads/eurofusion/WPMST1PR15_13808_submitted.pdf.
24. Rosato, J., Marandet, Y., and Stamm, R. 2017. A new table of Balmer line shapes for the diagnostic of magnetic fusion plasmas. *Journal of Quantitative Spectroscopy and Radiative Transfer*, 187, 333-337. Available online: http://www.euro-fusionscipub.org/wp-content/uploads/WPMST1PR16_16415_submitted.pdf.
25. Seaton, M. J. "Atomic data for opacity calculations. XIII. Line profiles for transitions in hydrogenic ions." *Journal of Physics B: Atomic, Molecular and Optical Physics* 23.19 (1990): 3255. Available online: https://iopscience.iop.org/article/10.1088/0953-4075/23/19/012/pdf?casa_token=v3E-mYXAsAYAAAAA:LHktDfgu3oet-NnK_D8mkxgGI6R3HBPXNL28PQB7eDrfuUE1motozE6L_djU5D26vDnOd5ihqxo.

Sample Availability: Samples of the compounds are available from the authors.